# Adsorption of Alkenes on Acidic Zeolites. Theoretical Study Based on the Electron Charge Density

**M. Fernanda Zalazar,[†,‡] Darío J. R. Duarte,[†] and Nélida M. Peruchena*[,†,‡]**

*Laboratorio de Estructura Molecular y Propiedades, Área de Química Física, Departamento de Química, Facultad de Ciencias Exactas, Naturales y Agrimensura, Universidad Nacional del Nordeste, Avenida Libertad 5460, (3400) Corrientes, Argentina, and Facultad Regional Resistencia, Universidad Tecnológica Nacional, French 414, (3500) Resistancia, Chaco, Argentina*

*Received: June 8, 2009; Revised Manuscript Received: September 10, 2009*

In the present work, experiments on electron density changes in the adsorption process of alkenes on acidic zeolites, in the framework of atoms in molecules theory (AIM), were carried out. Electron densities were obtained at MP2 and B3LYP levels using a 6-31++G(d,p) basis set. This study explores the energetic and the electron density redistributions associated with O−H···$\pi$ interactions. The main purpose of this work is to provide an answer to the following questions: (a) Which and how large are the changes induced on the molecular electron distribution by the formation of adsorbed alkenes? (b) Can a reasonable estimate of the adsorption energy of alkenes on the active site of zeolite be solely calculated from an analysis of the electron densities? We have used topological parameters to determine the strength and nature of the interactions in the active site of the zeolite. All the results derived from the electron density analysis show that the stabilization of the adsorbed alkenes follows the order isobutene > *trans*-2-butene ≅ 1-butene ≅ propene > ethene, reflecting the order of basicity of C═C bonds, i.e., ($C_{ter}$═$C_{prim}$) > ($C_{sec}$═$C_{sec}$) ≅ ($C_{prim}$═$C_{sec}$) > ($C_{prim}$═$C_{prim}$). In addition, we have found a useful set of topological parameters that are good for estimating the adsorption energy in adsorbed alkenes.

## 1. Introduction

Zeolites are microporous aluminosilicate minerals that are widely used in industry as solid acid/base catalysts. They possess a network of cavities and channels that allow them to accommodate relatively large molecules such as hydrocarbons. They are framework silicates consisting of interlocking tetrahedrons of SiO4 and AlO4, where the presence of tetrahedral Al in its chemical structure gives rise to very high acidic properties and constitutes what are called acidic zeolites. Because of their high selectivity, their reactivity, and the presence of Brønsted acid sites, the acidic zeolites act as catalysts in a variety of industrial processes.[1] The alkene adsorption process on acid zeolites represents a step of several catalytic reactions of great industrial importance such as dimerization, isomerization, polymerization, and cracking processes.

The adsorption of alkenes on zeolites has been experimentally studied using Fourier transform infrared (FTIR) spectroscopy, NMR spectroscopy, and other methods.[2−8] The observed shift in the O−H and C═C bond vibrational stretching frequency, after the interaction of the alkene with the bridged hydroxyl group, has been used as a measurement of the strength interaction between the Brønsted acid sites and the alkenes. In addition, extensive theoretical studies have been done in order to understand the nature of the bonds involved in the adsorption process and the mechanisms of the reactions between the catalyst and the alkenes. These studies are mainly based on Mulliken's charge analysis, on structural and energetic parameters, and on vibrational frequency analysis.[9−18] In general, these studies concluded that the adsorption process does not significantly perturb the structure of either the adsorbed molecule or the zeolite itself. This is due to the strength of the interactions between the hydrocarbons and the zeolite. For small cluster models, the adsorbed molecules are $\pi$-bonded to the active site of the Brønsted acid site (with almost equal bond distances between the two double-bond carbons and the Brønsted proton), being this interaction either a hydrogen bond or an electrostatic one, according to the author.[9−18] Summing up, the nature of the adsorbed complex has been largely studied and remains a subject of discussion. A large discrepancy in calculated adsorption energy values is observed.[12,19−21] In consequence, the information available for these systems is far from complete.

In order to make a contribution to the field, the aim of the present work was to profoundly study the electron density changes experienced in the adsorption process. This study is related to previous ones that are based on the topological distribution of the electron charge density in carbocationic species involved in acid-catalyzed alkane transformations.[22−25] It is also related to another one based on the protonation reaction of ethene on acidic zeolites.[26]

The electronic density is a real physical property of a molecular system. Its experimental determination by high resolution X-ray diffraction is time-consuming. This is a fact even today with all the technical and methodological improvements that are observed in the experimental field such as the use of synchrotron radiation at low temperatures and better area detectors.[27] Within the rigorous principles of quantum mechanics, the electron density, an observable physical property, can be calculated at a correlated level and can provide quantitative information on atomic as well as intra- and intermolecular bonding properties.[28]

Therefore, the contribution of the theoretical calculations of electron density to answering the questions raised about acid

* Corresponding author. E-mail: peruchen@exa.unne.edu.ar.
† Universidad Nacional del Nordeste.
‡ Universidad Tecnológica Nacional.

10.1021/jp9053814 CCC: $40.75 
Published on Web 11/04/2009

catalysis on zeolites is important. Unlike alkanes, which only exhibit $\sigma$-electron delocalization, the alkenes exhibit the possibility of $\sigma$- and $\pi$-electron delocalization. In consequence, and in order to understand the structural and electronic factors involved in the stabilization of adsorbed alkenes, we considered it interesting to investigate the electron density distribution characteristics in adsorbed alkenes where the double bond is established between carbons of different natures ($C_{prim}$=$C_{prim}$, $C_{prim}$=$C_{sec}$, $C_{sec}$=$C_{sec}$ and $C_{prim}$=$C_{ter}$).

Calculations have been performed on ethene, propene, 1-butene, *trans*-2-butene, and isobutene adsorbed on an acidic zeolite cluster (T5-OH). A topological study of the electronic charge density distribution in the context of the atoms in molecules quantum theory (QTAIM) proposed by Bader[29] is applied in the present study. Using this approach, the nature of different interactions between the acid zeolite and the alkene and their relative contribution to the total adsorption energy can be seen.

A fundamental aspect of this work is based in the profound study of the principal contribution to the adsorption energy in adsorbed alkenes (O−H···$\pi$ interaction) by the distribution topology of the charge density. Additionally, we wanted to show that the topological analysis of the electronic charge density is a powerful tool to deeply study the strength and the nature of the interactions that are present between the catalyst and the alkene.

Previously, Rozas et al.[30] studied other chemical systems where F−H···$\pi$ interactions were analyzed using the electronic charge density. They have theoretically shown that the nature of the interactions present in the complexes formed between hydrogen fluoride and a series of $\pi$-systems is an F−H···$\pi$ H-bond one. Similar results were obtained, by Novoa and Mota,[31] for C−H···$\pi$ and O−H···$\pi$ interaction types. In addition, Zhang et al.[32] have also investigated Cl−H···$\pi$ interactions in the ethene−HCl complex. These X−H···$\pi$ hydrogen bonds, where X = C, O, F, and Cl, can be considered as types of hydrogen bond links between an HX bond (in the donor molecule) pointing to the $\pi$-electron density of the carbon−carbon double bond.

As we mentioned before, in the case of alkenes adsorbed to zeolites (and in view of the particular characteristics of a zeolite of being a strongly solid acid[1]), we consider of particular interest the characterization of the O−H···$\pi$ interaction in order to determine its strength and nature. Furthermore, we wanted to highlight the differences in the O−H···$\pi$ interaction properties when compared with other similar X−H···$\pi$ bond types.

In many of their works, Bader et al. have shown that topological parameters derived from the atoms in molecules theory correlated better with the hydrogen bond energy than with the geometric parameters.[33] Together, with the parameters mentioned above, the electron charge density and the Laplacian show correlations to the strength of the hydrogen bonds.[34−36] In order to characterize the O−H···$\pi$ interaction in adsorbed alkenes to zeolites, criteria based on the topological analysis of the electron density proposed by Koch and Popelier[37,38] are used.

Our results show that the O−H···$\pi$ interaction between the alkene and the acidic zeolite can be considered to be an unusual hydrogen bond with moderate strength. The interaction strength based on charge density values follows the order isobutene > *trans*-2-butene ≅ 1-butene ≅ propene > ethene. In addition, energetic parameters, based on electron density, show that the stabilization of the adsorbed alkenes is related to the nature of the double bond of alkenes following the same order: isobutene > *trans*-2-butene ≅ 1-butene ≅ propene > ethene.

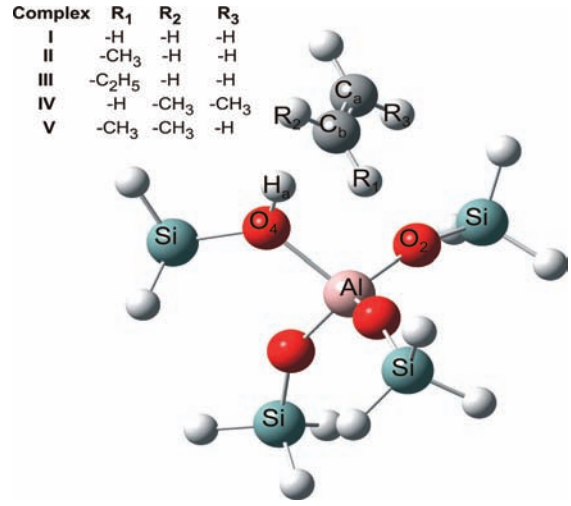


**Figure 1.** Optimized geometries of the structures of $\pi$ complex or alkene adsorbed, in which the alkene molecule interacts via its $\pi$ electrons with the hydrogen atom of the bridged hydroxyl group of the Brønsted acid site of a zeolite cluster.

Information obtained from the topological analysis of the electron charge density is essential to better understanding the interactions between species involved in alkene adsorption to zeolites.

## 2. Method and Calculation Details

We selected five alkene molecules as candidates for the study of alkene adsorption on zeolites: ethene, propene, 1-butene, *trans*-2-butene, and isobutene. This set of molecules is useful for considering the different natures of the olefinic carbons. The zeolite catalyst has been modeled by a widely used cluster, $H_3Si-OH-Al(-O-SiH_3)_3$, denoted T5-OH, because this model provides a good description of the bifunctional nature of zeolite active sites and includes, as far as possible, the electrostatic effects of short and medium range.[19,26]

The geometries of all species were optimized without any constraint, except for the Si−H distances. Hybrid density functional theory calculations at the Becke3 Lee−Yang−Parr (B3LYP) level[39] with the 6-31G** basis set were carried out with the Gaussian 03 suite of programs.[40] All stationary points were characterized by calculating the Hessian matrix and analyzing the vibrational normal modes.

The topological analysis of the electron charge density distribution in the framework of the atoms in molecules theory (AIM)[28,29,38] has been carried out for the present study. Total electron densities were obtained at B3LYP and MP2 levels with the 6-31++G** basis set. The bond and atomic properties were calculated using the Aim2000 package.[41] Analysis of charge transference between orbitals was performed using Weinhold's natural bond orbitals (NBO) theory[42] and the NBO 3.1 program[43] as implemented in Gaussian 03.

## 3. Results and Discussion

**3.1. Characterization of the O−H···$\pi$ Interaction in Adsorbed Alkenes.** Generally, it is accepted that the interaction of the alkene double bond with the zeolite Brønsted acid site results in the formation of an adsorbed alkene. This compound is more stable than the separated reactants due to the O−H···$\pi$ interaction. Figure 1 schematically shows the structure of an adsorbed alkene in which the alkene molecule interacts via its $\pi$ electrons with the hydrogen atom of the bridged hydroxyl group of the Brønsted acid site of a zeolite cluster.

**TABLE 1: Optimized Geometric Parameters of Adsorbed Olefins Calculated at B3LYP/6-31G(d,p) Level**

| | distance (Å) | | | | | | | bond angles (deg) | | |
|---|---|---|---|---|---|---|---|---|---|---|
| complex | $O_4-H_a$[a] | $H_a\cdots C_a$ | $H_a\cdots C_b$ | $H_a\cdots\pi$[b] | $O_4\cdots C_a$ | $O_4\cdots C_b$ | $O_4\cdots\pi$[c] | $O_4-H_a\cdots C_a$ | $O_4-H_a\cdots C_b$ | $O_4-H_a\cdots\pi$[d] |
| I | 0.9811 | 2.2316 | 2.2426 | 2.1398 | 3.1375 | 3.1478 | 3.0757 | 153.00 | 152.87 | 158.93 |
| II | 0.9848 | 2.1448 | 2.2763 | 2.1122 | 3.1205 | 3.1904 | 3.0888 | 170.64 | 153.93 | 171.02 |
| III | 0.9852 | 2.1733 | 2.2444 | 2.1049 | 3.1548 | 3.1374 | 3.0738 | 174.05 | 150.13 | 167.37 |
| IV | 0.9862 | 2.1752 | 2.1938 | 2.0787 | 3.1160 | 3.1527 | 3.0616 | 159.00 | 163.76 | 174.33 |
| V | 0.9889 | 2.0718 | 2.3000 | 2.0838 | 3.0572 | 3.1990 | 3.0559 | 174.18 | 150.44 | 167.12 |

[a] In isolated cluster of $O_4-H_a$ distance is 0.9697 Å. [b] Geometric distance from $H_a$ atom to the center of $C_a=C_b$ double bond. [c] Geometric distance from $O_4$ atom to the center of $C_a=C_b$ double bond. [d] Angle between $O_4$, $H_a$ atoms and the center of $C_a=C_b$ double bond.

Table 1 lists some of the optimized geometric parameters of adsorbed complexes calculated at the B3LYP/6-31G(d,p) level. The I, II, III, IV, and V complexes correspond to ethene, propene, 1-butene, *trans*-2-butene, and isobutene, respectively, adsorbed on the cluster T5-OH. From the analysis of Table 1, it is clear that when the alkene is symmetrical (i.e., ethene and *trans*-2-butene) the Brønsted acid proton of the zeolitic cluster, $H_a$, is located practically at the same distance from both double bond carbon atoms, whereas in complexes II, III, and V, the $H_a$ atom is located near the primary carbon atom, $C_a$.

The results displayed in Table 1 show that the $H_a\cdots C_a/C_b/\pi$ distances lie between 2.1 and 2.3 Å, the $O_4\cdots C_a/C_b/\pi$ distances lie between 3.1 and 3.2 Å, and the $O_4-H_a\cdots C_a/C_b/\pi$ angles lie in the range of 150−174°. In agreement with the classification of the hydrogen bond strength, based on geometric parameters,[44] it can be seen that, independently of how the interaction is considered, $H_a\cdots C_a$, $H_a\cdots C_b$, or $H_a\cdots\pi$, in all species studied in this work a hydrogen bond of moderate strength is formed.

The charge density $\rho_{(r)}$ is a physical quantity that has a definite value at each point in space. According to the AIM theory,[29] an atom in a molecule is defined as the union of an attractor and its associated basin, called an atomic basin. It is bounded by a zero-flux surface in the gradient vector field of the charge density, $\nabla\rho_{(r)}$, which defines an atomic boundary. When two atoms share some portion of their surfaces, a line of maximum electronic charge density is formed between the nuclei, and, at the point where the shared surface intersects this atomic interaction line or bond path there is a saddle point in $\rho_{(r)}$ called a bond critical point (BCP). In this manner, the AIM theory identifies a unique line of communication between two chemically interacting nuclei, and provides a unique point where it is possible to probe or characterize the interaction.[29] The network of the bond path (BP) linking pairs of neighboring nuclear attractors is called a molecular graph. Calculated properties at the BCP are labeled with the subscript "b" throughout this work.

Figure 2 shows the molecular graphs for ethene, propene, 1-butene, *trans*-2-butene, and isobutene adsorbed on the cluster T5-OH. The interactions responsible for the binding between fragments (organic and cluster) in adsorbed olefins originate atomic interaction lines (bond paths in the equilibrium structure) with the characteristics we will describe below.

In complexes I and IV, the acidic proton of the zeolite points to the center of the $C_a=C_b$ double bond. The $H_a\cdots\pi$ bond path, shown in Figure 2a,d, terminates at the BCP of the $C_a=C_b$ bond rather than in a nuclear attractor, whereas in complexes II, III and V, the $H_a\cdots\pi$ bond path is directed toward one of the carbon atoms of the double bond. As a result, in complexes II, III, and V the $H_a\cdots\pi$ bond path is highly curved in the vicinity of the $C_a=C_b$ bond, as can be seen in Figure 2b,c,e.

It is interesting to highlight that in complexes I and IV, due to the alkene symmetry, the length of the $H_a\cdots\pi/C_a$ bond path is shorter than in the other complexes. In consequence, the interaction of the $H_a$ atom in symmetrical alkenes takes place with the center of the $\pi$-cloud of the alkene, while in asymmetrical alkenes the interaction of the $H_a$ atom is established with the most hydrogenated carbon atom, $C_a$.

Table 2 reports the topological properties at the BCPs corresponding to the interactions $O_4-H_a\cdots\pi_{CC}$ (the bond path length (BPL), the electron densities ($\rho_b$), the Laplacian ($\nabla^2\rho_b$), the ellipticity ($\varepsilon$), and the relationship between the perpendicular and parallel curvatures ($|\lambda_1|/\lambda_3$). Along with the local kinetic energy density ($G_b$), the local potential energy density ($V_b$), and the total energy density ($E_{e(b)}$)), it also shows the properties at the BCPs for $C_a=C_b$ and $O_4-H_a$ bonds; these last two will be discussed later. Two calculation levels are reported for comparison.

Based on the AIM theory, Koch and Popelier proposed a set of eight topological criteria[37,38] for the existence of H-bonding. We investigated whether these criteria are also fulfilled for the principal interaction between the Brønsted acid proton of the zeolitic cluster and the double bond of the alkenes molecules, $H_a\cdots\pi_{CC}$.

The first criterion is the existence of a BCP between the hydrogen of the proton donor bond and an acceptor with an electron density and Laplacian of the charge density characteristic value. The typical range of $\rho_b$ values for H-bonding is between 0.002 and 0.040 au, and the typical range of $\nabla^2\rho_b$ values is between 0.02 and 0.15 au (second and third criteria). It can be observed in the molecular graphs (Figure 2) that BCPs and linking bond paths between the $H_a$ atom of the zeolite cluster and the $\pi$-system of the alkene are found in all complexes, consistent with the first criteria. Additionally, Table 2 shows that the $\rho_b$ and $\nabla^2\rho_b$ values for $H_a\cdots\pi_{CC}$ interactions are in the proposed range.

The fourth condition concerns mutual penetration of the hydrogen of the proton donor and the acceptor atoms. Penetration takes place when the difference between nonbonded and bonded radii for both H atom ($\Delta r_H$) and acceptor ($\Delta r_B$) atoms are positive. Table 3 shows the corresponding results and indicates that, in all complexes, this penetration is positive. The mutual penetration values vary between 1.04 (in complex I) and 1.12 Å (in complex IV). Then the criterion of mutual penetrations is verified.

The following four Popelier's criteria used to characterize hydrogen bonds refer to atomic properties integrated[45] over the hydrogen atomic basin. These properties are shown in Table 4 and are as follows: the average number of electrons, $N_{(\Omega)}$; the atomic energy, $E_{(\Omega)}$; the atomic net charge, $q_{(\Omega)}$; the atomic volume, $v_{(\Omega)}$; and the first moment of the atomic charge distribution, $M_{(\Omega)}$. This last property measures the extent and direction of the dipolar polarization undergone by the atomic density as a consequence of the $O-H\cdots\pi_{CC}$ interactions. The accuracy of the integration was assessed by the magnitude of a

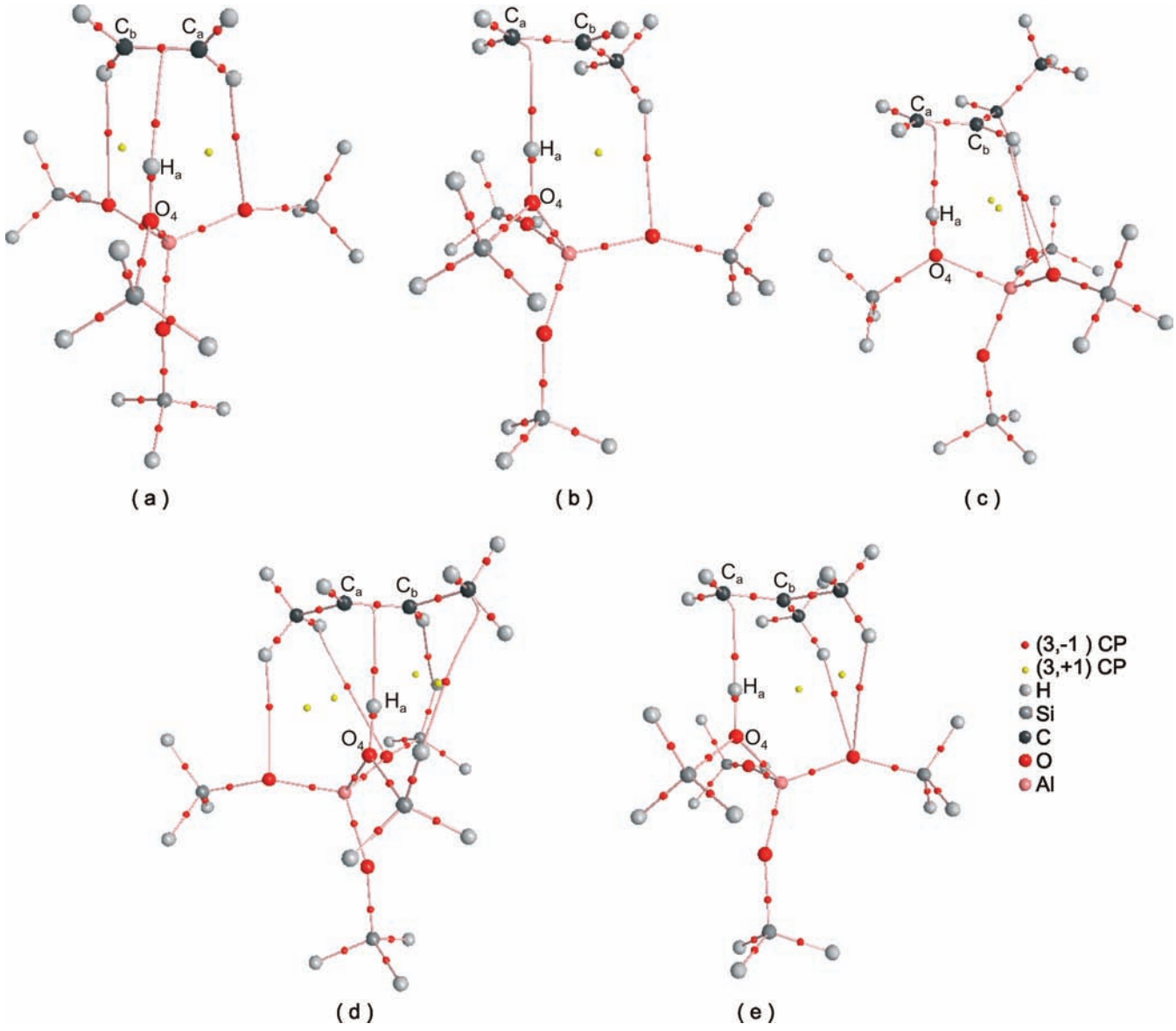


**Figure 2.** Molecular graphs for (a) ethene (b) propene, (c) 1-butene, (d) *trans*-2-butene, and (e) isobutene, respectively, adsorbed on the cluster T5-OH. Big circles correspond to attractors attributed to nuclei, lines connecting the nuclei are the bond paths, and the small red circles on them are the BCPs.

function $L(\Omega)$, which in all cases is less than $10^{-5}$ au for H atoms and $10^{-4}$ au for other atoms.

The fifth condition is the loss of electron population of the hydrogen atom from the proton donor. In all species studied here, we observed that this criterion was not satisfied. The following conditions are related to the energetic destabilization and the decrease of the dipolar polarization of the hydrogen of the proton donor. The results in Table 4 show that the energetic destabilization is always positive, $\Delta E_{(H)} > 0$, ranging from 0.0034 to 0.0044 au, which agrees with the typical destabilization for hydrogen atom in H-bonding. On the other hand, in complexes I, II, III and IV an increase in the dipole moment was produced; this is in disagreement with the seventh criterion established by Popelier. In complex V the dipole moment shows no significant change.

The last criterion is the decrease of the atomic volume of the hydrogen atom from the proton donor. In Table 4 it can be observed that $v_{(H)}$ decreases in all cases when the complex is formed, fulfilling Popelier's criterion. Nevertheless, this result is not in agreement with the increase of the electronic population. It is interesting to highlight that when the complexes are formed the hydrogen atom increases its electronic population and displays a volume contraction.

The criterion related to the mutual penetrations of the hydrogen and the acceptor atom has proven to be a *sufficient criterion* to conclude that a hydrogen bond is present, whereas the other criteria were deemed as *necessary*.[37,38] In summary, by consideration of Popelier's criteria, the $O_4-H_a\cdots\pi_{CC}$ interactions found in adsorbed alkenes of zeolite acid sites do not fulfill all Popelier's criteria. However, the *sufficient criterion* of mutual penetration of the hydrogen and the acceptor atom is clearly fulfilled by all interactions. In consequence, they can be considered as unusual hydrogen bonds.

The main purpose of the present work is the investigation of the still unexplained abnormality found in adsorbed alkene complexes on acidic zeolites, in order to provide an answer to the following questions:

1. Which and how large are the changes induced on the molecular electron distribution by the formation of adsorbed alkenes?

**TABLE 2: Local Topological Properties (in au) of the Electron Charge Density Distribution Calculated at the Position of the Bond Critical Points of Selected Bond Paths for Complexes I, II, III, IV, and V and for Isolated Cluster[a,b]**

| level | bond | complex | BPL | $\rho_b$ | $\nabla^2\rho_b$ | $\varepsilon$ | $\lvert\lambda_1\rvert/\lambda_3$ | $G_b$ | $V_b$ | $E_{e(b)}$ |
|---|---|---|---|---|---|---|---|---|---|---|
| B3LYP | $H_a\cdots\pi_{CC}$ | I | 2.0790[c] | 0.0201 | 0.0448 | 0.8474 | 0.2820 | 0.0105 | −0.0098 | 0.0007 |
| | | II | 2.3339[d] | 0.0225 | 0.0447 | 0.5500 | 0.2976 | 0.0111 | −0.0111 | 0.0001 |
| | | III | 2.4462[d] | 0.0221 | 0.0446 | 0.6547 | 0.2971 | 0.0109 | −0.0106 | 0.0003 |
| | | IV | 1.9909[c] | 0.0233 | 0.0465 | 0.8420 | 0.3091 | 0.0114 | −0.0111 | 0.0003 |
| | | V | 2.1643[d] | 0.0255 | 0.0464 | 0.3262 | 0.3057 | 0.0125 | −0.0134 | −0.0009 |
| | $C_a{=}C_b$ | I | 1.3365 | 0.3439 | −1.0052 | 0.3409 | 2.6105 | 0.1330 | −0.5173 | −0.3843 |
| | | | (1.3301) | (0.3483) | (−1.0330) | (0.3598) | (2.7582) | (0.1363) | (−0.5309) | (−0.3946) |
| | | II | 1.3395 | 0.3421 | −0.9896 | 0.3538 | 2.5619 | 0.1323 | −0.5121 | −0.3797 |
| | | | (1.3329) | (0.3472) | (−1.0196) | (0.3733) | (2.7145) | (0.1365) | (0.5279) | (−0.3914) |
| | | III | 1.3416 | 0.3417 | −0.9866 | 0.3476 | 2.5347 | 0.1321 | −0.5108 | −0.3787 |
| | | | (1.3329) | (0.3470) | (−1.0183) | (0.3688) | (2.6970) | (0.1364) | (−0.5273) | (−0.3910) |
| | | IV | 1.3438 | 0.3409 | −0.9727 | 0.3686 | 2.5088 | 0.1329 | −0.5090 | −0.3761 |
| | | | (1.3368) | (0.3461) | (−1.0036) | (0.3892) | (2.6599) | (0.1371) | (−0.5250) | (−0.3880) |
| | | V | 1.3465 | 0.3393 | −0.9678 | 0.3557 | 2.4775 | 0.1310 | −0.5039 | −0.3729 |
| | | | (1.3364) | (0.3453) | (−1.0017) | (0.3810) | (2.6457) | (0.1362) | (−0.5228) | (−0.3866) |
| | $O_4{-}H_a$ | I | 0.9439 | 0.3341 | −1.9456 | 0.0125 | 1.1386 | 0.0696 | −0.6255 | −0.5560 |
| | | II | 0.9481 | 0.3301 | −1.9012 | 0.0127 | 1.1294 | 0.0699 | −0.6152 | −0.5452 |
| | | III | 0.9485 | 0.3296 | −1.8990 | 0.0124 | 1.1296 | 0.0697 | −0.6142 | −0.5445 |
| | | IV | 0.9498 | 0.3286 | −1.8822 | 0.0126 | 1.1254 | 0.0703 | −0.6112 | −0.5409 |
| | | V | 0.9528 | 0.3253 | −1.8212 | 0.0126 | 1.1192 | 0.0704 | −0.6036 | −0.5332 |
| | | | (0.9315) | (0.3495) | (−2.0700) | (0.0108) | (1.1716) | (0.0684) | (−0.6543) | (−0.5859) |
| MP2 | $H_a\cdots\pi_{CC}$ | I | 2.1396[c] | 0.0196 | 0.0452 | 0.8473 | 0.2713 | 0.0108 | −0.0104 | 0.0005 |
| | | II | 2.3497[d] | 0.0218 | 0.0457 | 0.5627 | 0.2849 | 0.0115 | −0.0116 | −0.0001 |
| | | III | 2.4732[d] | 0.0215 | 0.0453 | 0.6609 | 0.2844 | 0.0112 | −0.0111 | 0.0001 |
| | | IV | 2.0851[c] | 0.0227 | 0.0471 | 0.8212 | 0.2968 | 0.0118 | −0.0117 | 0.0000 |
| | | V | 2.1784[d] | 0.0246 | 0.0482 | 0.3487 | 0.2908 | 0.0129 | −0.0137 | −0.0008 |
| | $C_a{=}C_b$ | I | 1.3374 | 0.3416 | −0.9986 | 0.3579 | 2.6651 | 0.1421 | −0.5338 | −0.3917 |
| | | | (1.3301) | (0.3459) | (−1.0241) | (0.3808) | (2.8116) | (0.1457) | (−0.5473) | (−0.4017) |
| | | II | 1.3414 | 0.3397 | −0.9809 | 0.3698 | 2.6044 | 0.1415 | −0.5282 | −0.3867 |
| | | | (1.3329) | (0.3448) | (−1.0101) | (0.3909) | (2.7595) | (0.1458) | (−0.5440) | (−0.3983) |
| | | III | 1.3416 | 0.3393 | −0.9783 | 0.3621 | 2.5839 | 0.1411 | −0.5269 | −0.3857 |
| | | | (1.3329) | (0.3445) | (−1.0096) | (0.3841) | (2.7467) | (0.1454) | (−0.5433) | (−0.3978) |
| | | IV | 1.3438 | 0.3385 | −0.9642 | 0.3811 | 2.5496 | 0.1420 | −0.5251 | −0.3831 |
| | | | (1.3351) | (0.3436) | (−0.9942) | (0.4030) | (2.7011) | (0.1463) | (−0.5411) | (−0.6873) |
| | | V | 1.3465 | 0.3368 | −0.9571 | 0.3703 | 2.5126 | 0.1401 | −0.5195 | −0.3794 |
| | | | (1.3364) | (0.3427) | (−0.9909) | (0.3961) | (2.6854) | (0.1454) | (−0.5385) | (−0.3931) |
| | $O_4{-}H_a$ | I | 0.9421 | 0.3302 | −1.9587 | 0.0131 | 1.1561 | 0.0770 | −0.6437 | −0.5667 |
| | | II | 0.9462 | 0.3262 | −1.9153 | 0.0132 | 1.1474 | 0.0770 | −0.6328 | −0.5558 |
| | | III | 0.9466 | 0.3258 | −1.9134 | 0.0130 | 1.1477 | 0.0768 | −0.6319 | −0.5551 |
| | | IV | 0.9479 | 0.3246 | −1.8959 | 0.0131 | 1.1432 | 0.0773 | −0.6286 | −0.5513 |
| | | V | 0.9509 | 0.3215 | −1.8666 | 0.0132 | 1.1378 | 0.0770 | −0.6207 | −0.5437 |
| | | | (0.9303) | (0.3454) | (−2.0607) | (0.0113) | (1.1795) | (0.0785) | (−0.6722) | (−0.5937) |

[a] To identify the atoms, see the text and Figure 2. [b] The values of the isolated species are included in parentheses. [c] Measured distance to the BCP of the $C_a{=}C_b$ bond. [d] Measured distance to the primary carbon $C_a$.

**TABLE 3: Mutual Penetration (in Å) of the Donor $H_a$ Atom and Acceptor B Atom for $H_a\cdots\pi$ Interaction[a]**

| complex | donor $H_a$ $\Delta r_H$ | acceptor B $\Delta r_B$ | total $\Delta r_H + \Delta r_B$ |
|---|---|---|---|
| I | 0.33 | 0.71 | 1.04 |
| II | 0.36 | 0.73 | 1.09 |
| III | 0.35 | 0.74 | 1.09 |
| IV | 0.36 | 0.76 | 1.12 |
| V | 0.39 | 0.71 | 1.10 |

[a] Symbols are explained in the text.

2. Can a reasonable estimate of the principal contribution to the adsorption energy (i.e., $O{-}H\cdots\pi$ interaction) of alkenes with the active site of the zeolite be derived from an analysis of electron densities only?

We would like to emphasize that such a comprehensive and deep analysis of the electron density has never been performed before in adsorbed alkenes on acidic zeolites. Thus, we will analyze in depth the topological properties of $O{-}H\cdots\pi$ interaction between different adsorbed alkenes on acidic zeolites.

The topological properties at the $H_a\cdots\pi$ BCP, in the complexes analyzed here, show that their $\rho_b$ values at B3LYP and MP2 levels (0.020−0.025 au) are lower (as is well-known) than the $\rho_b$ values found in covalent bonds (10 times lower than the C−H bond BCP). However, they are larger that those reported for other conventional $O{-}H\cdots\pi$ interactions considered weak hydrogen bonds (i.e., 0.011 au for $C_2H_4/H_2O$ complex[31,46] and 0.013 au for $C_3H_8/H_2O$ complex[46] at MP2/6-311++G(2d,2p) level and 0.010 au for $C_2H_2/H_2O$ complex at MP2/6-311++G(d,p)).[34] Also, our $\rho_b$ values results are even larger than that reported by Rozas et al. for $F{-}H\cdots\pi$ interaction in the $C_2H_4$/HF complex ($\rho_b = 0.0161$ au).[30]

For a more appropriate assessment, a topological analysis of $O{-}H\cdots\pi$ interactions in model systems ($C_2H_4/H_2O$ and $C_2H_4/CH_3OH$ complexes) was performed at the same computational level as the one used in adsorbed alkenes. These model system complexes are shown in Figure S1 of the Supporting Information, and the most important geometric and topological parameters are given in Tables S1−S3 of the Supporting Information. From the analysis of these results, we observed once more that the properties at the $H\cdots\pi$ BCP in adsorbed alkenes indicate

**TABLE 4: Topological Atomic Properties[a] (in au) of Selected Atoms in Adsorbed Alkenes[b,c]**

| atom | complex | $N_{(\Omega)}$ | $E_{(\Omega)}$ | $q_{(\Omega)}$ | $v_{(\Omega)}$ | $\lvert M_{(\Omega)}\rvert$ |
|---|---|---|---|---|---|---|
| $H_a$ | I | 0.369 | −0.3159 | +0.631 | 15.75 | 0.146 |
| | II | 0.372 | −0.3158 | +0.628 | 15.02 | 0.144 |
| | III | 0.371 | −0.3157 | +0.629 | 15.13 | 0.143 |
| | IV | 0.373 | −0.3168 | +0.627 | 14.46 | 0.142 |
| | V | 0.374 | −0.3161 | +0.626 | 14.59 | 0.141 |
| | | (0.353) | (−0.3202) | (+0.647) | (18.22) | (0.141) |
| $O_4$ | I | 9.518 | −75.6101 | −1.518 | 119.26 | 0.188 |
| | II | 9.516 | −75.6198 | −1.516 | 119.58 | 0.185 |
| | III | 9.516 | −75.6271 | −1.516 | 118.86 | 0.187 |
| | IV | 9.514 | −75.6276 | −1.514 | 118.89 | 0.191 |
| | V | 9.518 | −75.6287 | −1.518 | 119.27 | 0.182 |
| | | (9.453) | (−75.5433) | (−1.453) | (117.61) | (0.245) |
| $C_a$ | I | 6.037 | −37.8547 | −0.037 | 93.94 | 0.077 |
| | | (6.014) | (−38.0557) | (−0.014) | (98.43) | (0.057) |
| | II | 6.065 | −37.8719 | −0.065 | 93.00 | 0.093 |
| | | (6.029) | (−38.0602) | (−0.029) | (99.11) | (0.071) |
| | III | 6.072 | −37.8763 | −0.072 | 95.21 | 0.086 |
| | | (6.032) | (−38.0586) | (−0.032) | (99.86) | (0.069) |
| | IV | 6.043 | −37.9008 | −0.043 | 77.67 | 0.048 |
| | | (6.016) | (−38.0858) | (−0.016) | (84.06 | (0.028) |
| | V | 6.088 | −37.8890 | −0.088 | 91.45 | 0.011 |
| | | (6.038) | (−38.0647) | (−0.038) | (99.41) | (0.084) |
| $C_b$ | I | 6.038 | −37.8562 | −0.038 | 93.71 | 0.080 |
| | | (6.014) | (−38.0557) | (−0.014) | (98.43) | (0.057) |
| | II | 6.017 | −37.8822 | −0.017 | 78.34 | 0.031 |
| | | (6.005) | (−38.0800) | (−0.005) | (84.03) | (0.028) |
| | III | 6.022 | −37.9086 | −0.022 | 75.53 | 0.045 |
| | | (6.010) | (−38.0933) | (−0.010) | (82.62) | (0.024) |
| | IV | 6.044 | −37.9001 | −0.044 | 78.17 | 0.055 |
| | | (6.015) | (−38.0854) | (−0.015) | (84.03) | (0.027) |
| | V | 6.009 | −37.9021 | −0.009 | 65.37 | 0.009 |
| | | (6.000) | (−38.0941) | (+0.000) | (71.07) | (0.032) |

[a] Atomic electron population, $N_{(\Omega)}$; total atomic energy, $E_{(\Omega)}$; net atomic charge, $q_{(\Omega)}$, atomic volume integrated to the 0.001 au external isodensity envelope, $v_{(\Omega)}$; atomic dipolar moment, $|M_{(\Omega)}|$ (all values in au). [b] For $M$, 1 au $\cong 8.478 \times 10^{-30}$ C m; for $E$, 1 au $\cong 2.6255 \times 10^{-3}$ kJ mol$^{-1}$. [c] The corresponding values of the isolated alkenes are included in parentheses.

that this interaction is stronger than in model system complexes (the higher the $\rho_b$ value at H···$\pi$ BCP, the higher the strength of the hydrogen bonded interaction).

In summary, based on the $\rho_b$ values, the $O_4-H_a\cdots\pi$ interaction between the $\pi$ electrons of the alkene molecule and the hydrogen atom of the bridged hydroxyl group of a Brønsted acid site of a zeolite is stronger than other similar O−H···$\pi$ interaction seen in simple systems. This result can be attributed to the acid strong character of the Brønsted acid site of the zeolite (i.e., T5−O−H···$\pi$ > F−H···$\pi$ > O−H···$\pi$).

Some correlations between topological and energetic parameters (well-established in simpler systems) were found for the T5-OH/alkene I−V complexes. For example, as was expressed above, the charge density values at H···$\pi$ BCP can be considered as a measurement of the strength of the interaction.[47] On the basis of these results, the relation follows the order isobutene > *trans*-2-butene ≅ 1-butene ≅ propene > ethene. In other words, the strength of the interaction is related to the nature of the double bond following the tendency ($C_{ter}$═$C_{prim}$) > ($C_{sec}$═$C_{sec}$) ≅ ($C_{prim}$═$C_{sec}$) > ($C_{prim}$═$C_{prim}$). This leads us to believe that the stabilization of the adsorbed alkene must be related to the basicity of the $\pi_{CC}$ bond in the same way that the stabilization of the carbocations[24] (formed in protonation of the alkanes) is in relation to the "$\sigma$-scale of basicity" proposed by Esteves et al.[48]

Furthermore, these findings lead us to look beyond the topological properties at H···$\pi$ BCP and further than the atomic properties on the hydrogen atom. Consequently, we have included, in the following section, an analysis of the redistribution of the C−C and O−H bond electron charge density, and the C and O atomic property changes that take place when forming the complex. This will allow us to understand the role that these bonds and atoms play in the formation and stabilization of the adsorbed complexes.

**3.2. Distribution of the Charge Density at C−C and O−H Bonds.** Table 2 shows that the topological properties at the BCP on $C_a-C_b$ and $O_4-H_a$ bonds are clearly indicative of shared interactions, namely, relatively large values for $\rho_b$ and negative values for $\nabla^2\rho_b$. The relationship $|\lambda_1|/\lambda_3$ is appreciably greater than 1 and $E_{e(b)}$ is large and negative. Finally, $G_b/\rho_b$ is less than 1 in all complexes and isolated species. The most important topological change observed in the formation of the $\pi$-complexes in adsorbed alkenes is the decrease of the electronic charge density of the BCPs at $C_a-C_b$ and $O_4-H_a$ bonds. These results are in accordance with the lengthening of both the $C_a-C_b$ and the $O_4-H_a$ bonds. Also, there is a smooth decrease in the Laplacian, the ellipticity, and the $|\lambda_1|/\lambda_3$ and $G_b/\rho_b$ relationships. With respect to the isolated alkenes, the electronic redistribution that accompanies the formation of the $\pi$-complex shows that the $C_a-C_b$ bond maintains its own double bond characteristics (with $\rho_b$ values between 0.3439 au in complex I and 0.3393 au in complex V and $\varepsilon$ values from 0.3409 to 0.3557, respectively). The C−C bond path length (BPL) slightly increased 0.0064 Å in complex I and 0.0100 Å in complex V. Furthermore, the magnitude or absolute value of $E_{e(b)}$ decreased at C−C BCP in adsorbed alkenes; this is indicative of a reduction of the covalent character, which is a consequence of the adsorption process.

The relative variation of $d$, $\rho_b$, and $\nabla^2\rho_b$ parameters ($\Delta P_{rel} = (P_{ads} - P_{isol})/P_{isol}$, with $P = d$, $\rho_b$, $\nabla^2\rho_b$) in the C−C bond were more significant in Laplacian values (the values lie between 2.7 and 3.4%). In a similar way, the same changes were found in the O−H bond in adsorbed alkenes with respect to isolated zeolite. Our results are consistent with a number of prior works[9−11] where it was reported that the O−H covalent bond in acid zeolites is stretched when engaged in an O−H···$\pi$ interaction. The distance relative variations are small (between 1.1 and 1.9%) in contraposition to the larger values of the relative variations in charge density and Laplacian and are indicative of the sensibility of these properties (from 4.4 to 6.9% and from 6.0 to 10.5%, respectively). In summary, the $\Delta P_{rel}$ in the Laplacian values is more significant than the $\Delta P_{rel}$ in the charge density values and is even more significant than the $\Delta P_{rel}$ in the distances values—for both bonds. Considering this, the variation in the Laplacian values at the BCP in the hydrogen donor bond is always considerably greater than that in the CC bond. This is in accordance with the idea that the proton donor molecules undergo more changes than the proton acceptor molecules in a hydrogen bond (HB) interaction.

Generally, it has been observed that the hydrogen bond energy provides a satisfactory correlation with the electronic density at H···A BCP.[34] However, other studies indicate that this correlation is better with local properties at D−H BCPs,[49] showing that an interesting point to measure the strength of the hydrogen bond would be the observation of the proton donor bond and the neighboring bonds (in our case, the acid site of the zeolite).

O−H···$\pi$ interactions formed in $C_2H_4/H_2O$ and $C_2H_4/CH_3OH$ complexes are weak HBs. However, T5-OH···$C_2H_4$ is not a weak interaction. What may be the explanation of this result? One possibility is that this could be a manifestation of the key role played by the hydrogen donor bond of acidic zeolites. It is

**TABLE 5: Sum of the Atomic Population in All Atoms of Alkene Fragments in Adsorbed and Isolated Species as well as the Difference between Both**

| | I | II | III | IV | V |
|---|---|---|---|---|---|
| 1 | 15.937 | 23.933 | 31.936 | 31.932 | 31.927 |
| 2 | (16.000) | (23.998) | (32.003) | (31.999) | (32.000) |
| $\Delta N_{(\text{alkene})}$[a] | 0.063 | 0.065 | 0.068 | 0.067 | 0.073 |

[a] Calculated as the difference between the sum of the atomic property in all atoms in isolated alkenes (2) and the same sum of the alkenes fragment in adsorbed alkenes (1).

also necessary to emphasize that acid zeolites are considered highly acidic solid-acid catalysts and strong hydrogen donors, whose acidity is comparable to superacid liquids.[1] The acidic strength of the Brønsted site of zeolites is attributable to the proton of the bridging hydroxyl group being bonded to an oxygen atom that is also linked to a silicon and to an aluminum, which makes the oxygen a tricoordinated atom. This tricoordinated oxygen confers to the proton of the bridging hydroxyl group its particular properties. As a consequence, it is reasonable to believe that the topological feature of the distribution of the charge density of the OH bond must be investigated in depth. Therefore, it is of particular interest to characterize the interactions between zeolites and $\pi$-cloud alkenes ($O_4-H_a\cdots\pi_{CC}$) and to know their properties in order to analyze similarities to or differences from other $X-H\cdots\pi$ bond types, which are considered weak hydrogen bonds. Accordingly, the results shown in Table 2 are indicative of the great change of the charge density distribution in O−H bonds due to the formation of hydrogen bonds.

In addition, the changes in the electronic distribution, which take place on the $\sigma$(OH) and $\pi$(CC) bonds in the formation of the adsorbed alkenes, are mirrored by the atomic properties. Following, Table 4 shows the topological atomic properties of selected atoms in the site of the interaction. Unfortunately, the size of the real system and the prohibitive computing time for the integrated atomic properties did not allow us to explore the contacts further than the inner layer of the active region modeled by a small cluster (T5-OH).

The most remarkable observation is that in all complexes studied here an increase of the electronic population in $H_a$, $O_4$, $C_a$, and $C_b$ atoms is observed. In spite of the unsatisfied criteria of the decrease of the $N_{(\Omega)}$ of the hydrogen atom, unexpectedly, the two carbon atoms involved in the CC double bond (considered the $\pi$-donor) do not display a significant decrease of the atomic populations. In other words, the $\Delta N_{(\Omega)}$ values are positive.

In order to understand these "odd" results, we have calculated the $\Delta N_{(\Omega)}$ in alkene fragments, expressed as the difference between the sum of the atomic population in all atoms in isolated alkenes and the same sum in adsorbed alkenes. These values are shows in Table 5 and will be discussed later. Furthermore, following the decrease in the atomic volume of the hydrogen atom, after their interaction with the $\pi$-cloud, $C_a$ and $C_b$ carbon atoms became more compact by volume contraction.

It is also noticeable that, when the interaction occurs, the carbon atoms that conceptually act as the $\pi$-donor system undergo an energetic destabilization, whether the oxygen atom is slightly stabilized as a consequence of this interaction. Moreover, the rearrangement of the electronic charge density within the atom is mirrored by the change in the atomic dipolar moment. A similar increased behavior in both carbon atoms is observed; the opposite occurs with the oxygen atom, where the dipolar moment is diminished by the interaction (see Table 4).

The results show that both carbon atoms have a slender negative charge, which slightly increases by the displacement of the charge density from the other hydrogen atoms of the alkenes (non-$H_a$ atom). The hydrogen atom has an important positive charge that, as was expressed before, does not undergo an augmentation during the interaction and the oxygen atom has an elevated negative charge. Notwithstanding this, the oxygen atom shows a augmentation of the negative charge as a consequence of the polarization that follows the HB formation, and as was previously stated, the hydrogen atom diminishes its positive atomic charge. In all cases, the changes in the atomic populations are small (i.e., the absolute difference is less than 100 me). We have previously seen that (in accordance with other cases where the charge transfer phenomenon is important), the electronic density is much more affected in the proton donor bond than in the proton acceptor bond.[50,51] In addition, the atomic properties of bonded hydrogen atoms are good estimators of interaction effects between the O−H bond and the $\pi$-cloud in the active site of the acidic zeolite. Considering that the hydrogen atoms (bonded and nonbonded) are weak attractors, with scarce electron charge density, then it is possible to believe that the electron charge within the hydrogen basin will be extremely suitable for a distortion and, in consequence, can be significantly affected by slight modifications of the molecular environment. Thus, in the next section, we have looked at hydrogen atoms aiming to give a detailed description of the $O-H\cdots\pi_{CC}$ interactions in the adsorption process.

**3.3. Laplacian of the Electron Charge Density at Hydrogen Atom.** Of particular interest for the present study is the Laplacian function of the electron density, $\nabla^2\rho$, the quantity at any point that determines the regions of the space where the electron density is locally concentrated or depleted.[52] The quantum shells of an atom are divided into an inner region where $\nabla^2\rho < 0$ and an outer one where $\nabla^2\rho > 0$. The portion of the shell where $\nabla^2\rho < 0$ is called the valence shell charge concentration (VSCC). Thus a local maximum (or minimum) in $-\nabla^2\rho$ signifies a local concentration (or depletion) of electron density.

According to the Koch and Popelier criteria, $\Delta N_{(H)}$ should be negative for hydrogen bonded complexes.[37,38] However, in other studied complexes that have been defined as hydrogen bonded (i.e., $F-H\cdots PH_3$), it was found that $\Delta N_{(H)}$ has a small and positive value. This was attributed to possible errors in the integration.[33] In this study we have found that complexes defined as hydrogen bonds also have a small and positive $\Delta N_{(H)}$, but we do not attribute this to a possible integration error. In consequence, and in addition to the criteria established by Popelier, we had also studied the distribution of the charge concentration on the hydrogen atoms. This can be done by analyzing the corresponding (3, −3) CP in the Laplacian around the hydrogen positions.[53]

Table 6 shows the maxima characterization (in $-\nabla^2\rho$) found near the nuclear position of the acidic hydrogen atom of the zeolite for adsorbed alkenes. The $-\nabla^2\rho$ value at the nuclear position is indicative of how large is the local accumulation of charge density in this point. As expected, an important decrease in the proton (3, −3) CP height (the value of the $-\nabla^2\rho$) of the bridging hydroxyl group was found in adsorbed alkene with respect to isolated acid zeolite. Our results show that the decrease of the charge concentration values of the bridge hydrogen nuclei in adsorbed isobutene (−1.0207 au) are larger than those in *trans*-2-butene (−0.8928 au), 1-butene (−0.8748 au), propene (−0.8500 au), and ethene (−0.7048 au). In other words, we observed that the strength of hydrogen bond correlates

**TABLE 6: Characterization of (3, −3) Critical Point of Laplacian for Acidic Hydrogen Atom ($H_a$) of the Zeolite in Complexes I−V[a]**

| complex | $-\nabla^2\rho$ | $r^b$ |
|---|---|---|
| I | 16.3105 | 0.0128 |
| II | 16.1652 | 0.0126 |
| III | 16.1404 | 0.0126 |
| IV | 16.1224 | 0.0125 |
| V | 15.9946 | 0.0124 |
| | (17.0152) | (0.0131) |

[a] The corresponding values for isolated species are included in parentheses. [b] $r$ is the distance (in au) from (3, −3) CP to the nucleus of the acidic hydrogen atom ($H_a$).

better with the Laplacian parameters at the bridged hydrogen atom (3, −3) CP than with the electron density at H···$\pi$ BCP parameters.

In order to compare to another known system, the decrease of the (3, −3) CP in the $CH_3OH/C_2H_4$ complex $-\nabla^2\rho$ value is even lower (−0.4125 au) than the decrease in the T5-OH/alkene complexes $-\nabla^2\rho$ values. Our results show that the reduction value of concentration of the electronic charge density over the bridged hydrogen in the acid site of the zeolite in the complexes studied here are about 50% higher than in the $CH_3OH/C_2H_4$ complex, resulting in a better stabilization of the alkenes adsorbed. Additionally, the decrease of a charge concentration at (3, −3) CP in bridged hydrogen atom is accompanied by the decrease of the distance from this critical point to the nuclear position. This diminution of the distance in adsorbed isobutene is greater than that in adsorbed ethene.

In summary, we have found that the decrease of the charge concentration on the hydrogen bonded atom, with respect to the nonbonded hydrogen atom, is an important indicator of the hydrogen bond strength in adsorbed alkenes.

**3.4. Energetic Interaction Studies from the Topological Properties. Estimation of the Total Contact Energy.** Several methodologies have been used for the theoretical determination of the adsorption energy due to its difficulty of experimental determination. Boronat et al.,[19] using a cluster similar to the one used in this study, informed that the isobutene adsorption energy is higher than the ethene one and it is still higher than the 1-butene one, with QM methods. Jousse et al. predicted the adsorption energies for butene isomers on silicalite zeolite using molecular dynamic simulations.[20] These energies are practically indistinguishable, but the trend is indicative of 1-butene > *trans*-2-butene = *cis*-2-butene > isobutene. In addition, Nieminen et al. have informed that the adsorption energy of ethene is less than that isobutene and it is still less than that of 1-butene using QM/MM studies.[12] Recently, Namuangruk et al. agreed that the calculated adsorption energies of the butene isomers are −16.06, −13.62, −13.25, and −6.96 kcal/mol for 1-butene, *cis*-2-butene, *trans*-2-butene, and isobutene, respectively, using two different ONIOM schemes.[21] Furthermore, the adsorption energy obtained by this method for ethene (−8.17 kcal/mol) resulted in an intermediate value between those of *trans*-2-butene and isobutene. In consequence, a large discrepancy in calculated adsorption energy values, depending the methodology, the cluster size, etc., is observed.

Our results display clearly lower values than those reported by other methodologies (−5.22, −6.24, −6.23, −6.26, and −6.93 kcal/mol for complexes I, II, III, IV, and V, respectively). However, considering that the adsorption energy can be partitioned into two contributions: the primary and principal contribution involves few atoms at the zeolite Brønsted acid site and the secondary contribution is due to the environment or to the action of the framework of the catalyst. Both contributions cannot be estimated in such a small cluster as the one utilized in this work; consequently only the primary contribution (defined as O−H···$\pi$ interaction and other C−H···O interactions at the zeolite bifunctional active site) was considered. Therefore, the fundamental aspect of this work is based on the in-depth study of the principal contribution to the adsorption energy in adsorbed alkenes by the distribution topology of the charge density. In other words, we would like to understand how the effect is produced by different alkenes (by differentiation of the characteristics of the carbon atoms involved in the double bond), in relation to the electron density changes experimented in the adsorption process.

Alternatively, many correlations between the hydrogen bond energy and the geometric parameters, (i.e., distance between donor−acceptor atoms, $d$(D···A); distance between hydrogen atom and hydrogen acceptor atom, $d$(H···A); or the distance between hydrogen atom and hydrogen donor atom, $d$(HD) (in other words, the hydrogen-donating covalent bond lengths)), are generally found in the literature.[54] Moreover, geometric parameters, such as bond distances and bond angles, hold little chemical information. However, if structural as well as electronic parameters, based on the molecular electronic density, are used for the characterization of these bonds, then we should be able to extract a maximum of chemical information.[55]

This information can be extracted from the experimental or calculated density within the rigorous field of quantum mechanics. For example, Espinosa et al. found that, despite different models, methods, and experimental conditions employed to obtain the BCP topological properties, $G_b$ and $V_b$ depend exponentially on the H···O distance.[56] In his paper and based in Abramov's approach (that allow the evaluation of the electronic kinetic energy density, $G_{(r)}$, from the knowledge of the experimental electron density only) Espinosa et al. have established a proportionality between the HB energy, $E_{HB}$ (theoretically determined), and the local potential energy density evaluated at H···A BCP, denoted $V_b$. The latter is in turn easily obtained from $G_b$, using the local statement of the virial theorem.[29]

$$\frac{\hbar^2}{4m}\nabla^2\rho_{(r)} = 2G_{(r)} + V_{(r)} \quad (1)$$

By the analysis of 83 experimentally observed HBs [D−H···O (D = C, N, O)], using accurate X-ray diffraction data, Espinosa et al. have established the $E_c = (1/2)V_b$ relationship, where $E_c$ is the contact energy or the (individual) HB energy.[56]

In consequence, to estimate the strength of the intermolecular interactions in adsorbed alkenes, we have used the relationship provided by Espinosa[56] for the calculation of the contact energy. This relationship is very important in cases such as those studied here because several atomic interactions are formed between both fragments.

In the molecular graph (Figure 2) it can be seen that several bond paths connect atoms from organic and zeolitic fragments. In consequence, several contacts should contribute to the adsorption energy in the active site. In effect, the contributions of all intermolecular contacts can be evaluated in the same way using Espinosa's relationship. Therefore, the sum of HB energies conduces to the total contact energy, $E_{TC}$. As can be expected, the highest individual contact energy is due to the $O_4-H_a\cdots\pi_{CC}$ interaction, denoted as the principal contact energy, $E_{pc}$. Following this, Figure 3 shows $E_{pc}$ and $E_{TC}$ values. In addition,

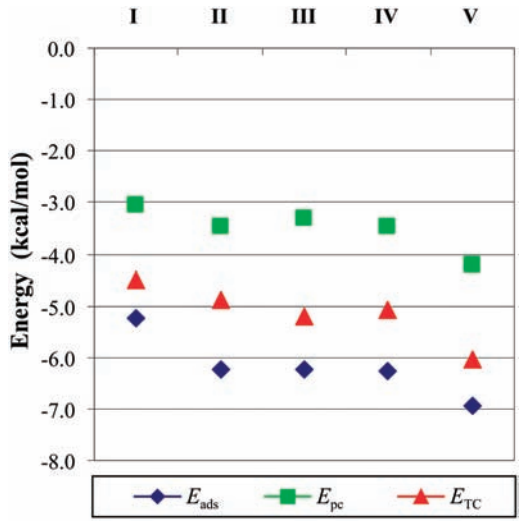


**Figure 3.** Principal contact energy $E_{pc}$, total contact energy $E_{TC}$, and adsorption energy $E_{ads}$ (kcal/mol) in adsorbed alkenes.

the adsorption energy values $E_{ads}$ (calculated as the difference between the complex energy and the sum of the isolated monomer energies) are also shown.

Our data analysis shows that the contact energy values for the $O_4-H_a\cdots\pi_{CC}$ interaction fall between −3.1 and −4.2 kcal/mol, which represent a contribution of 68−71% to the total contact energy. The individual contact energy values observed in the other C−H···O interactions (between organic and zeolitic fragments) are smaller and will not be discussed in this work. However, the results indicate that, in accordance with the initial expectations, the biggest contribution to the total energy is due to the interaction between the tricoordinated hydroxyl group (at the acid site of the zeolite) and the $\pi$-cloud from the alkene. Nevertheless, despite the rather small C−H···O interaction energy values, they significantly contribute to the adsorption energy at the active site of the catalyst.

Three calculated energies ($E_{ads}$, $E_{pc}$, and $E_{TC}$) show that the stabilization of the adsorbed species relates to the nature of the double bond of alkenes following the order isobutene > *trans*-2-butene ≅ 1-butene ≅ propene > ethene. In other words, the three of them follow the same tendency ($C_{ter}$=$C_{prim}$) > ($C_{sec}$=$C_{sec}$) ≅ ($C_{prim}$=$C_{sec}$) > ($C_{prim}$=$C_{prim}$).

**3.5. Relationship between the Adsorption Process Energy and Charge Transferred (by Charge Density Analysis).** In previous works we have shown the importance of the AIM studies in conjunction with the natural bond orbital (NBO) analysis of charge transference, in weak, moderate, and strong hydrogen bonds.[50] Both methodologies provide a good complement in the understanding of the intra- and intermolecular interactions. Subsequently, we have also calculated the charge transferred from the $\pi_{(CC)}$ bonding orbital (electron donor) toward the $\sigma^*_{(OH)}$ antibonding orbital (electron acceptor).

The amount of charge transferred, $\Delta n$, taking place during the interaction of alkenes with an acid zeolite is presented in Table 7. As a result, the stabilizing interaction (two orbitals−two electrons) between a $\pi_{(CC)}$ *donor* orbital and a $\sigma^*_{(OH)}$ *acceptor* orbital is analyzed using natural bond orbital (NBO) analysis. The energetic stabilization, $\Delta E^{(2)}$, due to the $\pi_{(CC)} \rightarrow \sigma^*_{(OH)}$ interaction, can be estimated by second order perturbation theory, where the characteristics of the filled (electron donor) orbital and the unfilled (electron acceptor) orbitals are specifically considered.

If $\Delta n_{CC\ donor} < 0$, and $\Delta n_{OH\ acceptor} > 0$, the charge flows from the double bond of the alkene to the OH antibonding orbital at the acid site of the zeolite. A relationship between the calculated adsorption energies and the $\Delta E^{(2)}$ and, again, between the calculated adsorption energies and the amount of charge transferred between both orbitals can be obtained.

**TABLE 7: Natural Bond Orbital Charge-Transfer Analysis of Complexes I−V at the B3LYP/6-31++G** Level of Theory[a]**

| complex | donor [$\pi_{(CC)}$] $\Delta n$ (me) | acceptor [$\sigma^*_{(OH)}$] $\Delta n$ (me) | $\Delta E^{(2)}[\pi_{(CC)} \rightarrow \sigma^*_{(OH)}]$ (kcal/mol) |
|---|---|---|---|
| I | −40.80 | 34.43 | 10.15 |
| II | −40.63 | 38.67 | 11.45 |
| III | −40.49 | 37.90 | 11.42 |
| IV | −38.75 | 38.14 | 11.30 |
| V | −40.28 | 43.58 | 12.45 |

[a] Populational variation, $\Delta n$, calculated as the difference between the adsorbed alkenes and the isolated species.

Beyond the charge transferred between orbitals provided by NBO analysis, we can estimate the total charge density transferred from the alkenes, in the context of the AIM theory, and relate this to the strength of the adsorption in different alkenes. The total electron charge density transferred is calculated as the alkene electron charge density loss during the adsorption process. In this way, the atomic population in all atoms of the alkene were calculated using Bader's partition.[45] In consequence, the difference between the total electron population of the adsorbed alkene and the isolated alkene ($\Delta N_{alkene}$) has been considered. Similarly to the NBO analysis, in the AIM analysis, if $\Delta N_{alkene} < 0$, then the electronic charge density will flow from the alkene to the zeolite. In other words, $\Delta N_{alkene}$ represents the fractional number of electrons transferred from the electron donor unit (alkene) to the electron acceptor unit (zeolite) in adsorbed alkenes, expressed in electron numbers. The values are reported in Table 5.

The maximum amount of charge transfer takes place between isobutene and T5-OH, whereas the minimum amount of charge flows between ethene and T5-OH. Moreover, the total charge transferred (AIM analysis) from the alkene to the catalyst shows a tendency similar to the charge transferred between orbitals (NBO analysis). In consequence, an additional parameter to the ones defined here can be used to estimate the "relative strength" of the main interaction displayed in the adsorption process. Indeed, it is important to consider (in contraposition to the atomic charge) that the AIM formalism proposed by Bader[29] is very consistent and is physically supported because the electronic density is pondered as the quantum-mechanical observable.

## 4. Conclusions

In the present work we have presented detailed calculations of the adsorption of ethene, propene, 1-butene, *trans*-2-butene, and isobutene on acidic zeolites. These alkene molecules act as test molecules for the study of the interaction between an olefinic hydrocarbon and the zeolite. We have obtained the geometric and energetic parameters as well as the charge transfer and topological properties of alkenes adsorbed on acidic zeolites by DFT and MP2 calculations. The Koch and Popelier criteria, commonly used to establish hydrogen bonds, have been applied for the first time in their entirety for the characterization of the interaction between the zeolite Brønsted acid sites and the alkenes involved in the adsorption process. An in-depth study of the electron density changes produced in the adsorption process was done in order to understand the nature of the principal contribution to the adsorption energy. We have

explored, additionally, the expressions proposed by Espinosa et al. to relate the potential energy densities $V_b$ to the H-bond strength, in order to estimate the adsorption energy at the active site of the catalyst and using topological properties. All results can be summarized as follows:

(i) The *sufficient criterion of mutual penetration* of the $H_a$ and the $\pi_{CC}$ acceptor atoms was *clearly fulfilled by all systems*. As a consequence, the $O-H\cdots\pi_{CC}$ interactions between the alkenes and the acidic zeolite can be considered as "unconventional types of hydrogen bond" with moderate strength. The interaction strength, based on charge density values, follows the order isobutene > *trans*-2-butene ≅ 1-butene ≅ propene > ethene.

(ii) The relative variations of the Laplacian values (at the BCP in bridging hydroxyl group) are more significant than the relative variations of the electronic density values and the relative variations of the bond length. This means that, in the systems studied here, the topological parameters such as the electronic density and the Laplacian at the proton-donating BCP are even more sensitive to the interaction with the $\pi$-cloud than the length of the OH bond.

(iii) Additionally, we have found that the decrease of the charge concentration (evaluated at the (3, −3) CP of the Laplacian topology, on the acidic hydrogen atom), caused by the formation of the adsorbed complex, is an important indicator of the strength of the hydrogen bond.

(iv) Energetic parameters, based on the electron density, indicate that the principal contribution to adsorption energies at the acid site of the zeolite is directly related to the stability of the $\pi$-complex and to the ability of the alkene atoms to transfer electron charge toward the zeolite.

(v) The total charge transferred (AIM analysis) from the alkene to the catalyst shows a tendency similar to the charge transferred between orbitals (NBO analysis). In consequence, an additional parameter can be used to estimate the relative strength of the adsorption process.

All the results derived from the electron density analysis show that the stabilization of the adsorbed alkenes follow the order isobutene > *trans*-2-butene ≅ 1-butene ≅ propene > ethene, reflecting the order of basicity of C=C bonds, i.e., $(C_{ter}=C_{prim}) > (C_{sec}=C_{sec}) \cong (C_{prim}=C_{sec}) > (C_{prim}=C_{prim})$. Finally, the present work has highlighted the potentialities that the electron charge density topological analysis (and their Laplacian) offer for the study of the principal contribution involved in the adsorption process on acid zeolites, in adsorbed alkenes.

**Acknowledgment.** The authors acknowledge SECYT UNNE for financial support. M.F.Z. is a research fellow of CONICET, D.J.R.D. is a research fellow of SECYT UNNE, and N.M.P. is a career researcher of CONICET, Argentina. This work was supported by Grant PICTO-UNNE 089.

**Supporting Information Available:** Figure S1 showing structures of $C_2H_4/H_2O$ and $C_2H_4/CH_3OH$ complexes and Tables S1−S3 giving the most important geometric and topological parameters. This material is available free of charge via the Internet at http://pubs.acs.org.

## References and Notes

(1) Corma, A. *Chem. Rev.* **1995**, *95*, 559.
(2) Cant, N. W.; Hall, W. K. *J. Catal.* **1972**, *25*, 161.
(3) Kondo, J. N.; Wakabayashi, F.; Domen, K. *J. Phys. Chem. B* **1998**, *102*, 2259.
(4) Yoda, E.; Kondo, J. N.; Domen, K. *J. Phys. Chem. B* **2005**, *109*, 1464.
(5) White, J. L.; Beck, L. W.; Haw, J. F. *J. Am. Chem. Soc.* **1992**, *114*, 6182.
(6) Spoto, G.; Bordiga, S.; Ricchiardi, G.; Scarano, D.; Zecchina, A.; Borello, E. *J. Chem. Soc., Faraday Trans.* **1994**, *90*, 2827.
(7) Trombetta, M.; Busca, G.; Rossini, S.; Piccoli, V.; Cornaro, U. *J. Catal.* **1997**, *168*, 349.
(8) Ivanov, P.; Papp, H. *Langmuir* **2000**, *16*, 7769.
(9) Boronat, M.; Viruela, P. M.; Corma, A. *J. Am. Chem. Soc.* **2004**, *126*, 3300.
(10) Kasuriya, S.; Namuangruk, S.; Treesukol, P.; Tirtowidjojo, M.; Limtrakul, J. *J. Catal.* **2003**, *219*, 320.
(11) Limtrakul, J.; Nanok, T.; Jungsuttiwong, S.; Khongpracha, P.; Truong, T. *Chem. Phys. Lett.* **2001**, *349*, 161.
(12) Nieminen, V.; Sierka, M.; Murzin, D. Y.; Sauer, J. *J. Catal.* **2005**, *231*, 393.
(13) Sauer, J.; Ugliengo, P.; Garrone, E.; Saunders, V. R. *Chem. Rev.* **1994**, *94*, 2095.
(14) Svelle, S.; Kolboe, S.; Swang, O. *J. Phys. Chem. B* **2004**, *108*, 2953.
(15) Benco, L.; Hafner, J.; Hutschka, F.; Toulhoat, H. *J. Phys. Chem. B* **2003**, *107*, 9756.
(16) Viruela, P.; Zicovich-Wilson, C. M.; Corma, A. *J. Phys. Chem. B* **1993**, *97*, 13713.
(17) O'Malley, P. J.; Farnworth, K. J. *J. Phys. Chem. B* **1998**, *102*, 4507.
(18) Pantu, P.; Boekfa, B.; Limtrakul, J. *J. Mol. Catal. A: Chem.* **2007**, *277*, 171.
(19) Boronat, M.; Zicovich-Wilson, C. M.; Viruela, P.; Corma, A. *J. Phys. Chem. B* **2001**, *105*, 11169.
(20) Jousse, F.; Leherte, L.; Vercauteren, D. P. *Mol. Simul.* **1996**, *17*, 175.
(21) Namuangruk, S.; Tantanak, D.; Limtrakul, J. *J. Mol. Catal. A: Chem.* **2006**, *256*, 113.
(22) Okulik, N. B.; Peruchena, N. M.; Esteves, P.; Mota, C.; Jubert, A. H. *J. Phys. Chem. A* **1999**, *103*, 8491.
(23) Okulik, N. B.; Peruchena, N. M.; Esteves, P. M.; Mota, C. J. A.; Jubert, A. H. *J. Phys. Chem. A* **2000**, *104*, 7586.
(24) Okulik, N. B.; Sosa, G. L.; Esteves, P.; Mota, C.; Jubert, A. H.; Peruchena, N. M. *J. Phys. Chem. A* **2002**, *106*, 1584.
(25) Okulik, N. B.; Peruchena, N. M.; Jubert, A. H. *J. Phys. Chem. A* **2006**, *110*, 9974.
(26) Zalazar, M. F.; Peruchena, N. M. *J. Phys. Chem. A* **2007**, *111*, 7848.
(27) Lobayan, R. M.; Sosa, G. L.; Jubert, A. H.; Peruchena, N. M. *J. Phys. Chem. A* **2005**, *109*, 181.
(28) Matta, C. F.; Boyd, R. J. *The Quantum Theory of Atoms in Molecules: From Solid State to DNA and Drug Design*; Wiley-VCH: Weinheim, 2007.
(29) Bader, R. F. W. *Atoms in Molecules. A Quantum Theory*; Oxford Science Publications, Clarendon Press: London, 1990.
(30) Rozas, I.; Alkorta, I.; Elguero, J. *J. Phys. Chem. A* **1997**, *101*, 9457.
(31) Novoa, J. J.; Mota, F. *Chem. Phys. Lett.* **2000**, *318*, 345.
(32) Zhang, Y.-H.; Hao, J.-K.; Wang, X.; Zhou, W.; Tang, T.-H. *J. Mol. Struct. (THEOCHEM)* **1998**, *455*, 85.
(33) Carroll, M. T.; Bader, R. F. W. *Mol. Phys.* **1988**, *65*, 695.
(34) Grabowsky, S. J. *Chem. Phys. Lett.* **2001**, *338*, 361.
(35) Wojtulewski, S.; Grabowski, S. J. *J. Mol. Struct.* **2002**, *605*, 235.
(36) Grabowski, S. J. *J. Phys. Org. Chem.* **2004**, *17*, 18.
(37) Koch, U.; Popelier, P. L. A. *J. Phys. Chem.* **1995**, *99*, 9747.
(38) Popelier, P. L. A. *Atoms in Molecules. An Introduction*; Pearson Education, Harlow, U.K., 2000.
(39) (a) Becke, A. D. *J. Chem. Phys.* **1993**, *98*, 5648. (b) Lee, C.; Yang, W.; Parr, R. G. *Phys. Rev. B* **1988**, *37*, 785.
(40) Frisch, M. J.; Trucks, G. W.; Schlegel, H. B.; Scuseria, G. E.; Robb, M. A.; Cheeseman, J. R.; Montgomery, J. A., Jr.; Vreven, T.; Kudin, K. N.; Burant, J. C.; Millam, J. M.; Iyengar, S. S.; Tomasi, J.; Barone, V.; Mennucci, B.; Cossi, M.; Scalmani, G.; Rega, N.; Petersson, G. A.; Nakatsuji, H.; Hada, M.; Ehara, M.; Toyota, K.; Fukuda, R.; Hasegawa, J.; Ishida, M.; Nakajima, T.; Honda, Y.; Kitao, O.; Nakai, H.; Klene, M.; Li, X.; Knox, J. E.; Hratchian, H. P.; Cross, J. B.; Adamo, C.; Jaramillo, J.; Gomperts, R.; Stratmann, R. E.; Yazyev, O.; Austin, A. J.; Cammi, R.; Pomelli, C.; Ochterski, J. W.; Ayala, P. Y.; Morokuma, K.; Voth, G. A.; Salvador, P.; Dannenberg, J. J.; Zakrzewski, G.; Dapprich, S.; Daniels, A. D.; Strain, M. C.; Farkas, O.; Malick, D. K.; Rabuck, A. D.; Raghavachari, K.; Foresman, J. B.; Ortiz, J. V.; Cui, Q.; Baboul, A. G.; Clifford, S.; Cioslowski, J.; Stefanov, B. B.; Liu, G.; Liashenko, A.; Piskorz, P.; Komaromi, I.; Martin, R. L.; Fox, D. J.; Keith, T.; Al-Laham, M. A.; Peng, C. Y.; Nanayakkara, A.; Challacombe, M.; Gill, P. M. W.; Johnson, B.; Chen, W.; Wong, M. W.; Gonzalez, C.; Pople, J. A. *Gaussian 03*, revision D.01; Gaussian, Inc.: Wallingford, CT, 2004.
(41) Blieger-König, F.; Schönbohn, J. *AIM 2000 program package*, version 2.0; Bader, R. F. W., chemical adviser; Büro fur Innovative Software Streibel Biegler-König: Bielefeld, Germany, 2002.

(42) Reed, A. E.; Curtiss, L. A.; Weinhold, F. *Chem. Rev.* **1988**, *88*, 899.
(43) Glendening, E. D.; Badenhoop, J. K.; Reed, A. E.; Carpenter, J. E.; Weinhold, F. *NBO Version 3.1*; Theoretical Chemistry Institute, University of Wisconsin: Madison.
(44) Steiner, T. *Angew. Chem., Int. Ed.* **2002**, *41*, 48.
(45) Bader, R. F. W. *Chem. Rev.* **1991**, *91*, 893.
(46) Vorobyov, I.; Yappert, M. C.; DuPré, D. B. *J. Phys. Chem. A* **2002**, *106*, 10691.
(47) Espinosa, E.; Alkorta, I.; Elguero, J.; Molins, E. *J. Chem. Phys.* **2002**, *117*, 5529.
(48) Esteves, P. M.; Alberto, G. G. P.; Ramírez-Solís, A.; Mota, C. J. A. *J. Am. Chem. Soc.* **1999**, *121*, 7345.
(49) Grabowski, S. J. *J. Phys. Chem. A* **2001**, *105*, 10739.
(50) Sosa, G. L.; Peruchena, N. M.; Contreras, R. H.; Castro, E. A. *J. Mol. Struct. (THEOCHEM)* **2002**, *577*, 219.
(51) Grabowski, S. J. *Hydrogen Bonding—New Insights*; Springer: Berlin, 2006.
(52) Popelier, P. L. A. *Coord. Chem. Rev.* **2000**, *197*, 169.
(53) Lobayan, R. M.; Sosa, G. L.; Jubert, A. H.; Peruchena, N. M. *J. Phys. Chem. A* **2004**, *108*, 4347.
(54) Jeferry, G. A. *An introduction to hydrogen bond*; Oxford University Press: New York, 1997.
(55) Popelier, P. L. A. *J. Phys. Chem. A* **1999**, *103*, 2883.
(56) Espinosa, E.; Molins, E.; Lecomte, C. *Chem. Phys. Lett.* **1998**, *285*, 170.

JP9053814